Time-resolved and excitation-dependent photoluminescence study of CdTe/MgCdTe double heterostructures grown by molecular beam epitaxy

Xin-Hao Zhao, Michael J. DiNezza, Shi Liu, Su Lin, Yuan Zhao, and Yong-Hang Zhang

Articles you may be interested in

Minority carrier lifetime of lattice-matched CdZnTe alloy grown on InSb substrates using molecular beam epitaxy
J. Vac. Sci. Technol. B **33**, 011207 (2015); 10.1116/1.4905289

Determination of CdTe bulk carrier lifetime and interface recombination velocity of CdTe/MgCdTe double heterostructures grown by molecular beam epitaxy
Appl. Phys. Lett. **105**, 252101 (2014); 10.1063/1.4904993

Growth, steady-state, and time-resolved photoluminescence study of CdTe/MgCdTe double heterostructures on InSb substrates using molecular beam epitaxy
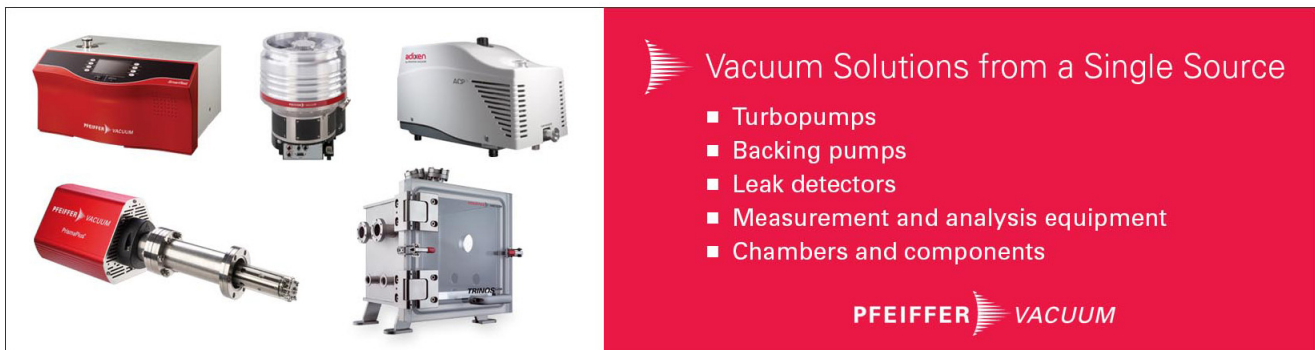Appl. Phys. Lett. **103**, 193901 (2013); 10.1063/1.4828984

Asymmetric AlAsSb/InAs/CdMgSe quantum wells grown by molecular-beam epitaxy
Appl. Phys. Lett. **84**, 4777 (2004); 10.1063/1.1759777

Effect of hydrostatic pressure on degradation of CdTe/CdMgTe heterostructures grown by molecular beam epitaxy on GaAs substrates
J. Appl. Phys. **89**, 5025 (2001); 10.1063/1.1360217

LETTERS

Time-resolved and excitation-dependent photoluminescence study of CdTe/MgCdTe double heterostructures grown by molecular beam epitaxy

Xin-Hao Zhao
Center for Photonics Innovation and School for Engineering of Matter, Transport, and Energy, Arizona State University, Tempe, Arizona 85287

Michael J. DiNezza and Shi Liu
Center for Photonics Innovation and School of Electrical, Computer, and Energy Engineering, Arizona State University, Tempe, Arizona 85287

Su Lin
Department of Chemistry and Biochemistry, Arizona State University, Tempe, Arizona 85287

Yuan Zhao and Yong-Hang Zhang[a]
Center for Photonics Innovation and School of Electrical, Computer, and Energy Engineering, Arizona State University, Tempe, Arizona 85287

This Letter reports the optical properties of CdTe/MgCdTe double heterostructures grown by molecular beam epitaxy. Low-temperature photoluminescence shows strong band-to-band emission and very weak defect related peaks, indicating low defect densities. The measured Shockley–Read–Hall lifetimes range from 57 to 86 ns at room temperature for samples grown under different conditions. The material radiative recombination coefficient B in the recombination rate defined as $R = A\Delta n + (1 - \gamma)B\Delta n^2 + C\Delta n^3$ [Wang *et al.*, Phys. Status Solidi B **244**, 2740 (2007)] is evaluated to be $4.3 \pm 0.5 \times 10^{-9}$ cm$^3 \cdot$s^{-1} with a photon recycling factor γ of 0.85 calculated based on the geometric structure of the samples. © *2014 American Vacuum Society.* [http://dx.doi.org/10.1116/1.4878317]

I. INTRODUCTION

Recently, there has been growing interest in the study of CdTe and related heterostructures with the goal of improving CdTe thin-film solar cells. CdTe has a nearly ideal bandgap (1.5 eV) and large absorption coefficient, which make it suitable for solar cell applications. Extensive studies were carried out on CdTe heterojunction solar cells,[1,2] and nowadays, polycrystalline p-type CdTe absorber and n-type CdS window layers grown on glass superstrate structures are used for thin-film cells with a record efficiency of 19.6%.[3] This efficiency is still much lower than the Shockley–Queisser limit (~32%) predicted by the detailed balanced model.[4] It is expected that monocrystalline CdTe enables higher efficiency solar cells due to much lower defect density. It can also be used as a model system to study not only novel high-efficiency cell designs but also various defects and grain boundaries in a controlled manner. With these motivations in mind, we recently demonstrated the molecular-beam-epitaxy (MBE) grown CdTe/MgCdTe double heterostructure (DH) with excellent structural and optical properties.[5] Furthermore, despite the extensive research on CdTe solar cells, the radiative recombination coefficient (B) is not well investigated. In this Letter, the optical properties, including the radiative recombination coefficient, of multiple CdTe/MgCdTe DHs are further investigated using low temperature photoluminescence (PL), time-resolved PL (TRPL), and excitation-dependent PL measurements.

II. EXPERIMENT

CdTe/MgCdTe DHs are grown on lattice matched (001) InSb substrates using a dual-chamber MBE system as reported previously.[5] The DHs consist of a 1 μm thick CdTe layer sandwiched by 30 nm thick MgCdTe barrier layers. All of the epilayers are undoped. It is found that MgCdTe provides sufficient carrier confinement for the CdTe layer, which enables PL measurements without significant surface recombination losses.[5]

PL measurements are carried out using a spectrometer equipped with a photomultiplier tube (PMT). The excitation source is a 532 nm laser diode. During excitation-dependent PL measurements, the laser power density is varied from 0.51 W/cm^2 to 118 W/cm^2 using a neutral density filter. The samples are mounted on the cold finger of a closed-cycle helium cryostat for temperature dependent measurements.

TRPL is measured using a time-correlated single photon counting (TCSPC) system. The excitation source is an ultrafast titanium-sapphire laser with a 130 fs pulse duration. The laser output at a wavelength of 750 nm is sent through a pulse selector to obtain pulses at a 0.8 MHz repetition rate. A

[a] Electronic mail: yhzhang@asu.edu

spectrometer equipped with a high speed microchannel plate PMT detector is used for single photon counting. The detection wavelength is set to 820 nm, which is the PL peak position of CdTe at room temperature. Data acquisition are done using a single photon counting card.

III. RESULTS AND DISCUSSION

At room temperature, all of the studied CdTe/MgCdTe DH samples show very strong PL intensity comparable to that of a MBE-grown GaAs/AlGaAs DH sample.[5] Temperature-dependent PL measurements are conducted under low laser power density (0.023 W/cm^2) for a CdTe/MgCdTe DH sample grown at 280 °C with Cd/Te flux ratio of 1.5. As shown in Fig. 1, the band edge emission peak shifts to higher energy as the temperature decreases. The slope of high energy side (the Planck tail) varies with temperature and is proportional to $1/kT$, as expected. The PL intensity is much stronger at lower temperatures due to weaker Shockley–Read–Hall (SRH) recombination. When the temperature reaches below 100 K, a broad peak in the range of 820–890 nm appears, which is believed to be related to defect states.[6] At higher temperatures, these defect states are more likely to recombine nonradiatively due to the interaction with phonons. Thus, this broad peak only shows up at very low temperatures. The intensity of the broad peak is more than two orders of magnitude weaker than that of the band edge emission, indicating low defect density in the CdTe layer and at the CdTe/MgCdTe interfaces.

Figure 2 shows the TRPL measurements of three CdTe/MgCdTe DH samples grown under different conditions. Samples A1561, A1564, and A1566 are grown with a Cd/Te flux ratio of 1.5 and substrate temperatures of 265 °C, 250 °C, and 295 °C, respectively. The initial photon excited carrier density in the CdTe layer is estimated to be less than 10^{15} cm^{-3}. The carrier decay dynamics can be modeled using the function, $\Delta n = \Delta n_0 \exp(-t/\tau)$, where Δn_0 is the initial excited carrier density and τ is the minority carrier

FIG. 2. (Color online) Time-resolved photoluminescence of CdTe/MgCdTe double heterostructures. Shockley–Read–Hall lifetime is extracted from the slope at the tail of the decay curve.

lifetime. For undoped epilayers, the measured lifetime is related to different recombination processes in the form of

$$\tau = \left(1/\tau_{\text{SRH}} + 1/\tau_{\text{Rad}} + 1/\tau_{\text{Aug}}\right)^{-1}$$
$$= \left(A + (1-\gamma)B(n_0 + \Delta n) + C(n_0 + \Delta n)^2\right)^{-1}, \quad (1)$$

where A, B, and C are the SRH, radiative, and Auger recombination coefficients, respectively. n_0 is the unintentionally doped carrier concentration. It is assumed that A is independent of the excess carrier densities. The radiative recombination coefficient B defined here is only dependent on the material properties such as the density of states and the optical transition matrix elements. γ is the photon recycling factor, which is the percentage of spontaneously generated photons reabsorbed by the CdTe layer.[7] Considering negligible effect of n_0 on the total lifetime, when Δn becomes sufficiently small, τ is approximately equal to the SRH lifetime. As shown in Fig. 2, the TRPL curves decay single-exponentially after 140 ns, and the SRH recombination lifetimes are extracted by fitting the single exponential decay part of the curves. The lifetime of the monocrystalline CdTe epilayers is much longer than that of typical polycrystalline CdTe films whose lifetime is only a few nanoseconds,[8] indicating that monocrystalline CdTe has much superior material properties. The longest lifetime of 86 ns is also longer than a recently reported 66 ns lifetime for a bulk monocrystalline CdTe measured by sub-bandgap two photon excitation method.[9]

Excitation-dependent PL measurements are conducted to analyze different recombination processes at different excitation levels and to extract the radiative recombination coefficient B. During steady-state PL measurements, the generation rate (G) is equal to the recombination rate (R) inside the CdTe layer as described by[7]

$$G = R = A\Delta n + (1-\gamma)B\Delta n^2 + C\Delta n^3. \quad (2)$$

In semiconductors, the large index of refraction results in a small escape cone for luminescence, and the large absorption coefficient near the bandedge ($\sim 2 \times 10^4$ cm^{-1})[10] results in a
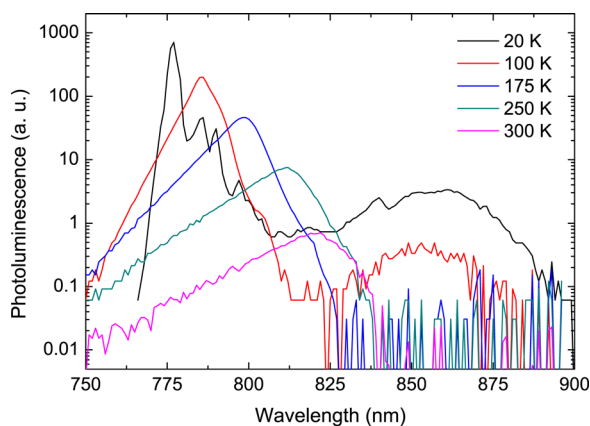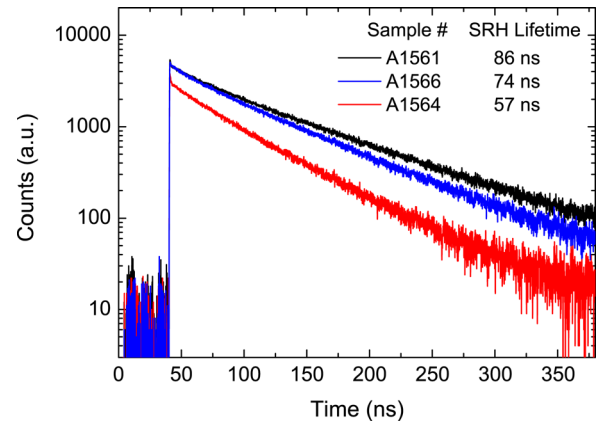

FIG. 1. (Color online) PL spectra of a CdTe/MgCdTe double heterostructure measured at different temperatures using the same excitation power density (0.023 W/cm^2). The band edge emission peak shifts to higher energy as temperature decreases. The PL intensity becomes stronger at lower temperatures indicating higher radiative recombination efficiency. The broad peak in the range of 820–890 nm at 20 K and 100 K is related to defect states.

short mean free path for photons created by radiative recombination inside the semiconductor. Consequently, the photons will either be recycled multiple times before escaping the sample (when the internal quantum efficiency is high) or will become heat through nonradiative recombination. It is therefore necessary to include the photon recycling effect, since it substantially affects the measured net radiative recombination rate when the internal quantum efficiency is relatively high. The photon recycling factor γ is calculated to be 0.85 for the 1 μm thick CdTe using the method introduced by Steiner *et al.*[11] The generation rate (G) is estimated based on the absorption of pump laser in the 1 μm CdTe layers, taking into account the reflection loss and loss in the front cap and barrier layers. The reflection loss is calculated based on the incident angle of laser and the refractive index of CdTe. No surface scattering is considered since the surface of the sample is specular. The relation in Eq. (2) is valid when photogenerated carrier density Δn is much larger than the equilibrium carrier density n_0. It is also assumed that recombination at the CdTe/MgCdTe interfaces is sufficiently small, and that carriers distribute uniformly in the CdTe layer. These assumptions are reasonable due to the fact that CdTe is undoped, has long carrier lifetime, and thus long diffusion length is expected. The measured PL intensity (I) is proportional to the net radiative recombination rate and can be expressed as

$$I = \eta(1 - \gamma)B\Delta n^2, \tag{3}$$

where η is a proportionality factor, which is affected by the collection efficiency of the spontaneous emission from the sample surface by the PL system. From Eqs. (2) and (3), the power law relation between the PL intensity (I) and generation rate (G) is given by[7]

$$G = A_0 I^{0.5} + B_0 I + C_0 I^{1.5}, \tag{4}$$

where $A_0 = A/\sqrt{\eta(1 - \gamma)B}$, $B_0 = 1/\eta$, and $C_0 = C/(\sqrt{\eta(1 - \gamma)B})^3$. The excitation-dependent PL results of the above three CdTe samples are shown in Fig. 3. The generation rate (G) is plotted as a function of the PL intensity (I) using a log–log scale. As shown in the figure, the sample with the longer SRH lifetime has a stronger PL intensity and therefore higher internal quantum efficiency compared to others at the same excitation density. For sample A1561, the slope of the curve is 0.52 at the low excitation range, which indicates that SRH recombination dominates at low injection according to the power law relation between G and I. This further confirms that the lifetime extracted from TRPL measurement at low excitation densities is the SRH lifetime. It also confirms that the equilibrium carrier density n_0 should be very low (estimated to be at least lower than 10^{15} cm^{-3}); otherwise, radiative recombination will contribute even under low excitation. As the generation rate becomes greater, the slope increases to 0.96, indicating that radiative recombination becomes dominant. No feature of Auger recombination was observed, which is expected since a relatively moderate PL pump density is used. All other CdTe
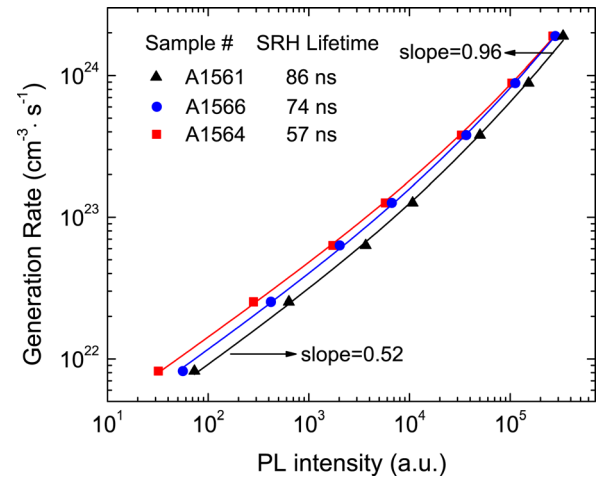

FIG. 3. (Color online) Excitation-dependent PL measurements of samples with different SRH lifetimes. At the same excitation rate, the sample with longer SRH lifetime shows stronger PL intensity. The slope of the curve for sample A1561 is 0.52 at lower excitation range meaning that SRH recombination dominates, whereas at higher excitation range the slope becomes 0.96, meaning that radiative recombination dominates.

samples demonstrated a similar behavior. Values of A_0 and B_0 are obtained by fitting the excitation-dependent PL curves with Eq. (4). The SRH recombination coefficient A is the inverse of the measured SRH lifetime, i.e., $A = 1/\tau_{SRH}$. Therefore, the radiative recombination coefficient (B) can be calculated using the relationship

$$B = \frac{A^2 B_0}{A_0^2(1 - \gamma)}, \tag{5}$$

which comes from Eqs. (3) and (4).

The published experimental values of the radiative recombination coefficient (B) are scattered according to the literature. Two references reported the values of B (2×10^{-9} cm$^3 \cdot$s^{-1} and 3×10^{-9} cm$^3 \cdot$s^{-1}) extracted from experimental results, without considering the photon recycling effect.[8,12] Thus, their reported B values are also related to the sample structure and may vary from sample to sample. In our work, the radiative recombination coefficient is defined as a material parameter, which is independent of sample geometry, since the geometry is accounted for by the photon recycling factor γ as defined above. Table I summarizes the fitting results for six CdTe DH samples grown under different conditions. The optimal growth temperature and CdTe flux ratio are 265 °C and 1.5, respectively, as determined by TRPL. As expected, similar values for material radiative recombination coefficient B are obtained despite different material qualities (i.e., different SRH lifetimes). The average radiative recombination coefficient of all the studied samples is then determined to be $4.3 \pm 0.5 \times 10^{-9}$ cm$^3 \cdot$s^{-1} for the MBE grown CdTe epilayers. It is worth of mentioning that accurate radiative recombination coefficient and the inclusion of photon recycling effect are critically needed for the modeling of CdTe solar cells.

IV. SUMMARY

In summary, the optical properties of six CdTe/MgCdTe double heterostructures grown under different conditions on

TABLE I. Summary of radiative recombination coefficient (B) of CdTe extracted from experimental results. A_0 and B_0 are obtained by fitting the excitation-dependent photoluminescence curves to Eq. (4) and B is calculated using Eq. (5) based on the measured SRH lifetime, A_0, B_0, and γ.

Sample #	Growth temperature ($^\circ$C)	Flux ratio (Cd/Te)	SRH lifetime (ns)	A_0 (cm$^{-3}\cdot$s^{-1})	B_0 (cm$^{-3}\cdot$s^{-1})	B (cm$^3\cdot$s^{-1})
A1561	265	1.5	86	8.78×10^{20}	3.74×10^{18}	4.3×10^{-9}
A1571	280	1.5	83	8.69×10^{20}	3.99×10^{18}	5.1×10^{-9}
A1566	295	1.5	74	1.12×10^{21}	4.63×10^{18}	4.5×10^{-9}
A1567	265	1.2	64	1.32×10^{21}	4.12×10^{18}	3.8×10^{-9}
A1568	265	1.8	58	1.45×10^{21}	3.95×10^{18}	3.7×10^{-9}
A1564	250	1.5	57	1.39×10^{21}	4.24×10^{18}	4.5×10^{-9}

lattice matched InSb substrates are studied with low temperature PL, time-resolved PL, and excitation-dependent PL measurements. SRH lifetimes ranging from 57 ns to 86 ns are measured at room temperature for these samples. Low temperature PL measurements show a strong band-to-band emission peak and a broad and much weaker defect related peak, indicating low defect density. With excitation-dependent PL measurements, it is found that SRH recombination dominates at low generation rate ($\sim 10^{22}$ cm$^{-3}\cdot$s^{-1}) and radiative recombination dominates at high generation rate ($\sim 10^{24}$ cm$^{-3}\cdot$s^{-1}). The sample geometry independent, material radiative recombination coefficient of CdTe is estimated to be $4.3 \pm 0.5 \times 10^{-9}$ cm$^3\cdot$s^{-1}, after corrected by the photon recycling effect. This parameter is needed for the modeling of CdTe solar cells.

ACKNOWLEDGMENTS

[1]A. Luque and S. Hegedus, *Handbook of Photovoltaic Science and Engineering* (John Wiley & Sons, Somerset, NJ, 2003), p. 617.
[2]X. Wu, Sol. Energy **77**, 803 (2004).
[3]M. A. Green, K. Emery, Y. Hishikawa, W. Warta, and E. D. Dunlop, Prog. Photovoltaics **21**, 827 (2013).
[4]A. P. Kirk, M. J. DiNezza, S. Liu, X.-H. Zhao, and Y.-H. Zhang, *Proceedings of the 39th IEEE Photovoltaic Specialists Conference*, Tampa, Florida, 16–21 June 2013, 2515–2517.
[5]M. J. DiNezza, X.-H. Zhao, S. Liu, A. P. Kirk, and Y.-H. Zhang, Appl. Phys. Lett. **103**, 193901 (2013).
[6]N. C. GilesTaylor, R. N. Bicknell, D. K. Blanks, T. H. Myers, and J. F. Schetzina, J. Vac. Sci. Technol., A **3**, 76 (1985).
[7]J.-B. Wang, D. Ding, S. R. Johnson, S.-Q. Yu, and Y.-H. Zhang, Phys. Status Solidi B **244**, 2740 (2007).
[8]R. K. Ahrenkiel, B. M. Keyes, D. L. Levi, K. Emery, T. L. Chu, and S. S. Chu, Appl. Phys. Lett. **64**, 2879 (1994).
[9]D. Kuciauskas, A. Kanevce, J. M. Burst, J. N. Duenow, R. Dhere, D. S. Albin, D. H. Levi, and R. K. Ahrenkiel, IEEE J. Photovoltaics **3**, 1319 (2013).
[10]S. Adachi, *Optical Constants of Crystalline and Amorphous Semiconductors: Numerical Data and Graphical Information* (Kluwer Academic, Boston, 1999), p. 530.
[11]M. A. Steiner, J. F. Geisz, I. García, D. J. Friedman, A. Duda, and S. R. Kurtz, J. Appl. Phys. **113**, 123109 (2013).
[12]R. Cohen, V. Lyahovitskaya, E. Poles, A. Liu, and Y. Rosenwaks, Appl. Phys. Lett. **73**, 1400 (1998).